Interface Focus (2012) 2, 746–756
doi:10.1098/rsfs.2012.0030
Published online 26 September 2012

Swarming and pattern formation due to selective attraction and repulsion

Pawel Romanczuk[1,*] and Lutz Schimansky-Geier[2,3]

[1]*Max Planck Institute for the Physics of Complex Systems, Nöthnitzerstrasse 38, 01187 Dresden, Germany*
[2]*Department of Physics, Humboldt Universität zu Berlin, Newtonstrasse 15, 12489 Berlin, Germany*
[3]*Instituto de Fìsica Interdisciplinar y Sistemas Complejos (IFISC), CSIC-UIB, Campus Universitat de les Illes Balears, 07122 Palma de Mallorca, Spain*

We discuss the collective dynamics of self-propelled particles with selective attraction and repulsion interactions. Each particle, or individual, may respond differently to its neighbours depending on the sign of their relative velocity. Thus, it is able to distinguish approaching (coming closer) and retreating (moving away) individuals. This differentiation of the social response is motivated by the response to looming visual stimuli and may be seen as a generalization of the previously proposed escape and pursuit interactions motivated by empirical evidence for cannibalism as a driving force of collective migration in locusts and Mormon crickets. The model can account for different types of behaviour such as pure attraction, pure repulsion or escape and pursuit, depending on the values (signs) of the different response strengths. It provides, in the light of recent experimental results, an interesting alternative to previously proposed models of collective motion with an explicit velocity–alignment interaction. We discuss the derivation of a coarse-grained description of the system dynamics, which allows us to derive analytically the necessary condition for emergence of collective motion. Furthermore, we analyse systematically the onset of collective motion and clustering in numerical simulations of the model for varying interaction strengths. We show that collective motion arises only in a subregion of the parameter space, which is consistent with the analytical prediction and corresponds to an effective escape and/or pursuit response.

Keywords: swarming; pattern formation; collective dynamics

1. INTRODUCTION

Collective motion in biology—as observed, for example, in flocks of birds, schools of fish or within bacterial colonies—is a fascinating display of natural self-organization. Over the years, it has been the topic of numerous scientific publications addressing it from very different angles and with different questions in mind, both experimentally and theoretically. From a more biological perspective, the interesting questions are the evolutionary advantages and the biological and ecological function of collective behaviour in various species [1–5], whereas physicist focus rather on universal laws and phase-transition behaviour by studying minimal models of collective motion [6–13]. The design, control and stability of collective dynamics in multi-agent systems is also a major research topic in engineering [14–17], and the general properties of related mathematical models are under active investigation in mathematics [18,19].

*Author for correspondence (prom@pks.mpg.de).

One contribution of 11 to a Theme Issue 'Collective motion in biological systems: experimental approaches joint with particle and continuum models'.

Most of the mathematical models for collective motion proposed in the literature contain some sort of explicit velocity-alignment mechanisms, which tends to align the velocity of a focal individual with the velocity of its neighbours [2,6,20–23]. However, recent experimental studies of collective behaviour in fish do not find any clear evidence for the existence of explicit velocity–alignment interactions [24,25]. Models with only attractive and repulsive interactions have long been studied in biology in the context of group formation and swarming [26–28]. Still, only relatively few models have focused on the onset of collective motion without alignment based on purely repulsive and attractive interactions [29–34]. This is most probably because velocity alignment provides a simple and robust mechanism for the onset of polarized swarms, where individuals are able to agree on a common direction of motion. For pure attraction and repulsion interactions, polarized motion is more difficult to obtain. In general, it requires an effective dampening out of velocity components associated with the relative motion of individuals. This might be achieved, for example, directly via dissipative interactions (inelastic collisions) [31,32] or an interaction-induced, nonlinear coupling of different velocity components of

Received 15 May 2012
Accepted 30 August 2012

self-propelled agents [30,33,35]. Although this 'physical' mechanisms yield very interesting results and can lead to coordinated motion of individual units, they are most probably not suited to explain the dynamics of many biological systems. In particular, they assume direct pairwise interaction forces, where the response of focal agent is accompanied by a 'mirror' response of its interaction partner, either directly as a result of the '*action* = *reaction*' principle for (social) forces defined by gradients of pair-wise interaction potentials, or because of dissipative interactions simultaneously acting on both agents.

Interestingly, the possibilities and potential restrictions on social response based on visual information have received only little attention in the context of collective motion (see recent studies [36,37] for notable exceptions). For example, growing or shrinking retinal images allow individuals to respond to their neighbour not only based on their spatial position (e.g. distance) but also based on their (relative) state of motion (e.g. approach versus movement away). This immediately implies the possibility of strongly asymmetric social interactions, which cannot be accounted for by gradients of pair-wise potentials.

Recently, motivated by empirical evidence for cannibalism as the driving force of collective migration in certain insect species [38,39], we have proposed a model of collective motion based on escape and pursuit responses [5,12]. In this escape–pursuit model, individuals react to their neighbours by moving away from others approaching them from behind (escape), and/or increasing their velocity towards those who are moving away in front of them (pursuit). This kind of social response requires individuals to distinguish between approaching and moving away (retreating) neighbours as well as between individuals in front and behind them. This previous model can be considered to belong to a broader class of selective attraction–repulsion models, which we believe are very promising for theoretical modelling of collective motion in biology. Please note that here we assume each individual being able to exhibit different responses to its neighbours based on their relative state of motion, which should be distinguished from the case of individuals with fixed behavioural roles such as predator and prey [40,41]. In this work, we discuss and analyse a generalization of the original escape–pursuit model to the case where self-propelled agents selectively respond to approach and movement away without differentiating between neighbours based on their relative position. Thus, we show that spatial anisotropy in social interactions is not essential for collective motion owing to selective attraction and repulsion. Furthermore, we do not put any restrictions on the sign (direction) of the effective social forces generating the selective response. This allows us to account for different social behaviour types, such as pure attraction, pure repulsion, and escape and pursuit, in a single model, by the same set of social forces, only by changing the values of the response strengths.

The model discussed here was first introduced in the context of collective motion and the evolution of density-dependent phenotypic plasticity in locusts [42]. However, on the basis of the above considerations, we believe it may be of relevance for various swarming phenomena mediated through visual information.

We will start with the definition of the individual-based model in terms of stochastic differential equations. Further on, we will briefly discuss the derivation of coarse-grained theory, which allows the formulations of evolution equations for the population-level variables such as spatial density and velocity fields. Finally, we will discuss simulation results with a particular focus on the emergence of large-scale collective motion.

2. INDIVIDUAL-BASED MODEL

We consider a system of N self-propelled agents (particles) in two spatial dimensions, which move with a constant speed s_0 in a spatial domain of size $L \times L$ with periodic boundary conditions. The interaction between particles is modelled as an effective social force $\mathbf{F}_i$. The evolution of the system is determined by equations of motion for the positions $\mathbf{r}_i$ and the polar orientation angles φ_i, which determine the direction of the heading unit vector $\mathbf{e}_{h,i}(t)$:

$$\dot{\mathbf{r}}_i = s_0 \mathbf{e}_{h_i}(t) = s_0 \begin{pmatrix} \cos\varphi_i(t) \\ \sin\varphi_i(t) \end{pmatrix}, \tag{2.1}$$

and

$$\dot{\varphi}_i = \frac{1}{s_0}(F_{i,\varphi} + \sqrt{2D_\varphi}\xi_\varphi(t)). \tag{2.2}$$

The temporal evolution of φ_i is determined by the turning of the individual i as a result of social interactions $F_{i,\varphi}$ and random (angular) fluctuations with the intensity D_φ. The (angular) social force is given by the projection of the total social force vector $F_{i,\varphi} = \mathbf{F}_i \mathbf{e}_{\varphi_i}$ on the angular degree of freedom with $\mathbf{e}_{\varphi_i} = (-\sin\varphi_i, \cos\varphi_i)$. The angular noise $\xi_\varphi(t)$ is Gaussian white noise with zero mean and vanishing temporal correlations.

The total social force is given by a sum of three components:

$$\mathbf{F}_i = \mathbf{f}_\mathrm{c} + \mathbf{f}_\mathrm{m} + \mathbf{f}_\mathrm{a}. \tag{2.3}$$

The first term represents a short-range repulsion responsible for collision avoidance. It reads

$$\mathbf{f}_\mathrm{c} = -\frac{1}{N_\mathrm{c}} \sum_{j=1}^{N} \mu_\mathrm{c}\, \hat{\mathbf{r}}_{ji}\, H(l_\mathrm{c} - r_{ji}), \tag{2.4}$$

with $\mu_\mathrm{c} \geq 0$ being a constant repulsive turning rate. The Heaviside function $H(l_\mathrm{c} - r_{ji})$ ensures that collision avoidance takes place only if the distance $r_{ji} = |\mathbf{r}_j - \mathbf{r}_i|$ between the focal individual i and the respective neighbour j is below the distance l_c. The total short-ranged, repulsive response is normalized by the number of individuals within the collision avoidance distance

$$N_\mathrm{c} = N_\mathrm{c}(t) = \sum_{i=1}^{N} H(l_\mathrm{c} - r_{ji}). \tag{2.5}$$

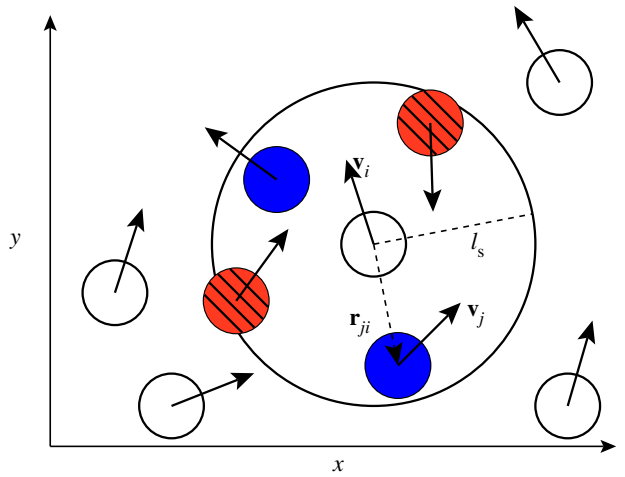

Figure 1. Schematic of social interactions: the focal individual i can interact with individuals within its sensory range l_s. Hereby, it distinguishes between 'approaching' (red/stripes) and 'moving away' (blue) individuals. The decisive factor in the distinction is the sign of relative velocity $\tilde{v}_{ji}$ defined by the projection of the velocity difference of neighbour j and the focal individual ($\mathbf{v}_{ji} = \mathbf{v}_j - \mathbf{v}_i$) on the relative position unit vector $\hat{\mathbf{r}}_{ji} = \mathbf{r}_{ji}/|\mathbf{r}_{ji}|$.

The other two forces read

$$\mathbf{f}_a = \frac{1}{N_a(t)} \sum_{j=1}^{N} \mu_a |\tilde{v}_{ji}| \hat{\mathbf{r}}_{ji} \times H(l_s - r_{ji}) H(r_{ji} - l_c) H(-\tilde{v}_{ji}), \tag{2.6}$$

and

$$\mathbf{f}_m = \frac{1}{N_m(t)} \sum_{j=1}^{N} \mu_m |\tilde{v}_{ji}| \hat{\mathbf{r}}_{ji} \times H(l_s - r_{ji}) H(r_{ji} - l_c) H(+\tilde{v}_{ji}). \tag{2.7}$$

Both forces represent averaged interactions with neighbouring agents, which act always along the unit vector pointing towards the centre of mass of the neighbour $\hat{\mathbf{r}}_{ji} = (\mathbf{r}_j - \mathbf{r}_i)/|\mathbf{r}_j - \mathbf{r}_i|$. The first one, $\mathbf{f}_a$, represents the response to approaching individuals characterized by a negative relative velocity $\tilde{v}_{ji} = (\mathbf{v}_j - \mathbf{v}_i)\hat{\mathbf{r}}_{ji} < 0$. The second, $\mathbf{f}_m$, is the corresponding response to moving away (retreating) individuals characterized by positive relative velocity $\tilde{v}_{ji} > 0$. Please note that the relative velocity depends on the velocity (direction of motion) of the focal individual as well as its neighbour. Based only on relative velocity, corresponding to the change of size of the retinal image, the focal individual may not distinguish who is moving away from whom. For example, if the focal individual itself moves away from a neighbour, the corresponding neighbour may be identified as 'retreating' even if it moves approximately in the direction of the focal individual (figure 1). In order to account also for this case and prevent any misunderstandings, we will mainly use the term 'moving away' instead of 'retreating', which is perhaps more appealing, while referring to the corresponding interaction. The differentiation based on the relative velocity is reflected by the last Heaviside functions $H(\pm\tilde{v}_{ji})$. The two other step functions are identical for both interactions and restrict these social responses to neighbours within a sensory range l_s but outside the repulsion zone. The parameters $\mu_{m,a}$ determine the turning rates owing to the respective interaction.

Both force terms are proportional to the relative velocity, which lead to a stronger response to faster approaching or receding individuals. Furthermore, they are normalized by the respective number of individuals for the corresponding interaction type:

$$\left.\begin{aligned} N_m(t) &= \sum_{i=1}^{N} H(r_{ji} - l_c) H(l_s - r_{ji}) H(+\tilde{v}_{ji}) \\ \text{and} \quad N_a(t) &= \sum_{i=1}^{N} H(r_{ji} - l_c) H(l_s - r_{ji}) H(-\tilde{v}_{ji}). \end{aligned}\right\} \tag{2.8}$$

Here, we used for simplicity step-like functions for the spatial dependence of the different interactions. The general results will not be altered by other smooth functions of the distance as long as they decay sufficiently fast in order to ensure local interactions. Please note that the definition of the step-like interaction zones resembles the two-zone model introduced by Couzin and co-workers [21,43]. However, the model discussed here does not contain an explicit velocity alignment.

Although variations in the relative strength and range of the collision-avoidance force ($\mathbf{f}_c$) may affect quantitatively the onset of collective motion, the qualitative behaviour of the model will not be affected by the short-ranged repulsion as long as $l_c \ll l_s$. Nevertheless, we keep it as it reflects the well-known tendency of individuals to keep a minimal distance to their neighbours and in addition prevents a population collapse for arbitrary choice of the other two—possibly attractive—social forces. However, in the following analysis, we will focus exclusively on the selective responses to approaching and moving away individuals.

Schematic of the interaction scheme with the differentiation between approach and movement away is given in figure 1.

The social forces $\mathbf{f}_{a/m}$ can lead independently to a repulsive (attractive) response to approaching individuals for $\mu_a < 0$ ($\mu_a > 0$) and a repulsion (attraction) to those moving away $\mu_m < 0$ ($\mu_m > 0$). In the $\mu_a\mu_m$-parameter space, we distinguish the four quadrants corresponding to different behaviour types (see also figure 2).

— *Pure repulsion.* Repulsion from approaching and moving away individuals: $\mu_a < 0$ and $\mu_m < 0$.
— *Escape and pursuit.* Repulsion from approaching individuals $\mu_a < 0$, attraction to moving away individuals $\mu_m > 0$.
— *'Head on head'.* Attraction to approaching individuals $\mu_a > 0$, repulsion from moving away individuals $\mu_m < 0$.
— *Pure attraction.* Attraction to approaching and moving away individuals: $\mu_a > 0$ and $\mu_m > 0$.

There exist also the special cases where there is no interaction with either approaching or moving away

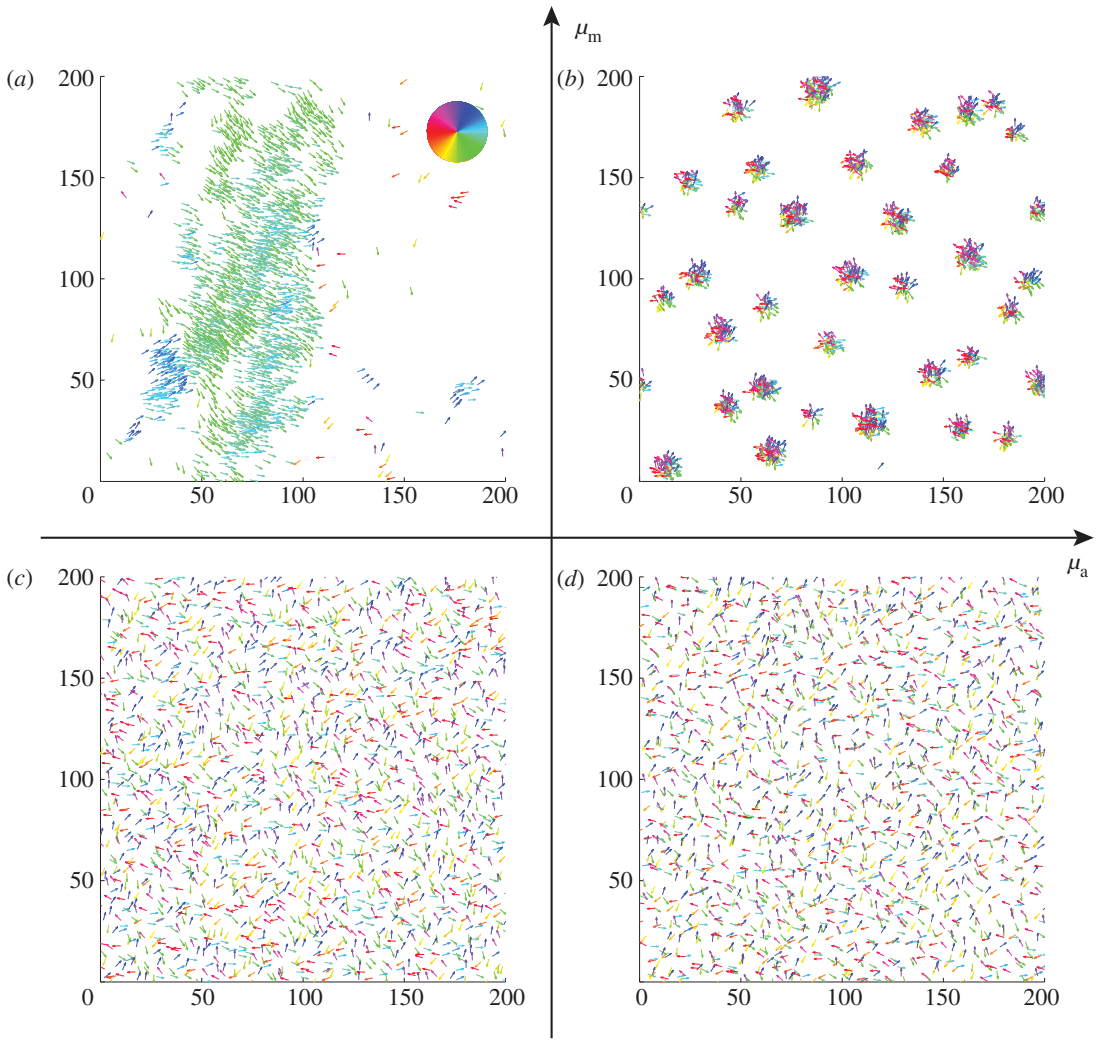

Figure 2. Examples of spatial configurations for different regimes: (*a*) 'escape and pursuit' ($\mu_a = -3.0$, $\mu_m = 3.0$); (*b*) 'pure attraction' ($\mu_a = 3.0$, $\mu_m = 3.0$); (*c*) 'pure repulsion' ($\mu_a = -3.0$, $\mu_m = -3.0$) and (*d*) 'head on head' ($\mu_a = +3.0$, $\mu_m = -3.0$). The arrows and their colour indicate the direction of motion of individual particles. The mapping of the colour to the directions is shown as an inset in panel (*a*). The different panels are arranged according to the location of the corresponding regime in the interaction parameter space, with the origin ($\mu_m = \mu_a = 0$) being in the centre.

Table 1. Summary of the model parameters with typical values used in simulations and corresponding dimensions in terms of arbitrary time t and space l units.

	parameter description	typical values used	unit
μ_m	response strength to moving away individuals	$-5 \ldots +5$	$1/t$
μ_a	response strength to approaching individuals	$-5 \ldots +5$	$1/t$
μ_c	collision-avoidance response strength	20	l/t^2
l_s	sensory range (range of social interactions)	5	l
l_c	diameter of the collision avoidance zone (short-ranged repulsion)	1	l
s_0	speed of individuals	1	l/t
D_φ	noise strength in the direction (angle) of motion of individuals	$0.02 \ldots 1.0$	l/t^2
L	system size (rectangular domain $L \times L$)	$100 \ldots 400$	l
N	number of individuals	2000	
$\mathrm{d}t$	numerical time step	0.005	t

individuals, i.e. $\mu_a = 0$ or $\mu_m = 0$. For example, for $\mu_m > 0$ ($\mu_m < 0$) and $\mu_a = 0$, the focal individual will be selectively attracted (repelled) by individuals moving away, but will ignore all approaching individuals.

We refer to the situation $\mu_a < 0$ and $\mu_m > 0$ as 'escape and pursuit', to due similar behaviour as in the original Brownian particle model [12]. For $\mu_a > 0$ and $\mu_m < 0$, the social forces lead to a preference to move towards other individuals that are already coming closer and therefore favour (in particular at low densities) frontal collisions between individuals. We refer to this regime as 'head on head'.

In table 1, we summarize the model parameters with typical values considered in this work.

3. COARSE-GRAINED DESCRIPTION

Starting from the microscopic, individual-based, description in terms of stochastic differential equations, it is possible to derive (approximate) evolution equations for coarse-grained observables, such as the spatial density of individuals and the corresponding average velocity field. Here, we can draw an analogy to the hydrodynamical theory of fluids. Although the behaviour of a fluid is determined by the dynamics and interaction of many individual molecules, we do need to 'follow' each of them in order to describe macroscopic flows. In fact, in most cases, this is entirely impossible as already a small droplet of fluid consists of an astronomically large number of molecules. Here, a coarse-grained hydrodynamic theory for macroscopic variables allows nevertheless the theoretical description of the system at time and length scales of interest.

In the context of swarming, there exist a number of works on the corresponding hydrodynamic theories of collective motion. Here, we should emphasize the seminal work by Toner & Tu [7,8], who first formulated a general hydrodynamic theory of swarming based purely on symmetry arguments.

In our case, the starting point for a derivation of a coarse-grained description is the introduction of the N-particle probability density function (PDF)

$$P_N(\mathbf{r}_1, \varphi_1; \mathbf{r}_2, \varphi_2; \ldots; \mathbf{r}_N, \varphi_N; t),$$

which determines the probability to find a particle (individual) at time t, at position $\mathbf{r}_i$, with velocity pointing in direction φ_i $(i = 1, 2, \ldots, N)$. It is normalized with respect to integration over space and over all angles.

For simplicity, one can assume that the N-particle PDF factorizes into a product of N one-particle PDFs, i.e. $P_N = \Pi_{i=1}^{N} P(\mathbf{r}_i, \varphi_i, t)$. In agreement with (2.1) and (2.2), we can write down the Fokker–Planck equation (FPE) for the PDF of the ith particle

$$\frac{\partial}{\partial t} P(\mathbf{r}_i, \varphi_i, t) = -\frac{\partial}{\partial \mathbf{r}_i} \mathbf{e}_{h_i} P - \frac{1}{s_0} \frac{\partial}{\partial \varphi_i} \mathbf{F}_i \mathbf{e}_{\varphi_i} P + \frac{D_\varphi}{s_0^2} \frac{\partial^2}{\partial \varphi_i^2} P, \tag{3.1}$$

with $\mathbf{e}_{h_i} = (\cos\varphi_i, \sin\varphi_i)^{\mathrm{T}}$ being the unit vector in the heading direction of individual i, and $\mathbf{e}_{\varphi_i} = (-\sin\varphi_i, \cos\varphi_i)^{\mathrm{T}}$ being the angular unit vector perpendicular to $\mathbf{e}_{h_i}$. The above FPE is nonlinear, because the interaction force $\mathbf{F}_i$ depends on the probability density for the position and the velocity angle of the particles within their sensory range.

The coarse-grained description can be now formally derived by using equation (3.1) to obtain equation of motion for the moments of the one-particle PDF, which are the particle density

$$\rho(\mathbf{r}_i, t) = \int_0^{2\pi} \mathrm{d}\mathbf{r} P(\mathbf{r}_i, \varphi, t), \quad \int_V \mathrm{d}\mathbf{r} \rho(\mathbf{r}_i, t) = 1, \tag{3.2}$$

and the expectation values of the cosine and sine of the velocity angle defined as

$$\left.\begin{aligned} s(\mathbf{r}_i, t) &= \int_0^{2\pi} \mathrm{d}\varphi \, \sin(\varphi) P(\varphi, t|\mathbf{r}_i) \\ \text{and} \qquad c(\mathbf{r}_i, t) &= \int_0^{2\pi} \mathrm{d}\varphi \, \cos(\varphi) P(\varphi, t|\mathbf{r}_i). \end{aligned}\right\} \tag{3.3}$$

where the conditional PDF of the velocity direction φ is defined through the relation $P(\mathbf{r}_i, \varphi, t) = P(\varphi, t|\mathbf{r}_i)\, \rho(\mathbf{r}_i, t)$. The moments in equation (3.3) represent space-dependent function that together fully determine the average velocity field $\mathbf{u}(\mathbf{r}_i, t) = s_0(s(\mathbf{r}_i, t), c(\mathbf{r}_i, t))$ of individuals at the spatial position $\mathbf{r}_i$, at time t.

A similar approach was previously used in the context of swarming of active Brownian particles in recent studies [44–46].

By combining the FPE (3.1) with the moment definitions (3.2)–(3.3) and integrating over the direction angle, we can derive after some analysis the evolution equation for these moments. In particular, one can obtain the equation for the so-called, coarse-grained order parameter $\Phi(\mathbf{r}_i, t) = \sqrt{s^2(\mathbf{r}_i, t) + c^2(\mathbf{r}_i, t)}$. The order parameter corresponds to the average velocity normalized by the speed of individuals s_0. It is 1 if all particles in the considered spatial region are perfectly aligned (ordered state) and tends to 0 if all particles move in different directions (disordered state).

The corresponding equation for the square of the order parameter reads

$$\begin{aligned} \frac{1}{2}\left\{\frac{\partial}{\partial t} + c(\mathbf{r}_i, t)\frac{\partial}{\partial x_i} + s(\mathbf{r}_i, t)\frac{\partial}{\partial y_i}\right\}\Phi^2(\mathbf{r}_i, t) \\ = -\frac{D_\varphi}{s_0^2}\Phi^2(\mathbf{r}_i, t) - \frac{1}{s_0}\big(c(\mathbf{r}_i, t)\langle\sin(\varphi_i)\mathbf{F}_i\mathbf{e}_{\varphi_i}\rangle \\ - s(\mathbf{r}_i, t)\langle\cos(\varphi_i)\mathbf{F}_i\mathbf{e}_{\varphi_i}\rangle\big) \\ - \frac{s_0 c(\mathbf{r}_i, t)}{\rho(\mathbf{r}_i, t)}\left\{\frac{\partial}{\partial x_i} T_{x_i,x_i}(\mathbf{r}_i, t)\rho(\mathbf{r}_i, t) + \frac{\partial}{\partial y_i} T_{x_i,y_i}(\mathbf{r}_i, t)\rho(\mathbf{r}_i, t)\right\} \\ - \frac{s_0 s(\mathbf{r}_i, t)}{\rho(\mathbf{r}_i, t)}\left\{\frac{\partial}{\partial x_i} T_{x_i,y_i}(\mathbf{r}_i, t)\rho(\mathbf{r}_i, t) + \frac{\partial}{\partial y_i} T_{y_i,y_i}(\mathbf{r}_i, t)\rho(\mathbf{r}_i, t)\right\}, \end{aligned} \tag{3.4}$$

where we used the following abbreviations:

$$\left.\begin{aligned} T_{x_i,x_i}(\mathbf{r}_i, t) &= \langle\cos^2(\varphi_i)\rangle - c^2(\mathbf{r}_i, t), \\ T_{x_i,y_i}(\mathbf{r}_i, t) &= \langle\cos(\varphi_i)\sin(\varphi_i)\rangle - c(\mathbf{r}_i, t)s(\mathbf{r}_i, t) \\ \text{and} \quad T_{y_i,y_i}(\mathbf{r}_i, t) &= \langle\sin^2(\varphi_i)\rangle - s^2(\mathbf{r}_i, t). \end{aligned}\right\} \tag{3.5}$$

The only term, which can induce an instability of the homogeneous disordered solution in equation (3.4), contains the interaction force. The remaining terms, which contain only the zeroth up to second moments of the orientation, are present also in the case of non-interacting particles. They describe the relaxation dynamics of $\Phi(t)$ towards a steady state, but are not the source of an eventual instability of the disordered solutions.

We note that, in order to obtain closed equations for the order parameter equation (3.4), one needs expressions for the expectation values containing the social force, as well as equations or expressions for the variances $T_{u_i.v_i}$.

In general, the treatment of the corresponding equations and integrals can be very tedious. Analytical solutions are often only possible by making a number of simplifying assumptions, which may strongly restrict the validity of the results. The corresponding calculations become quite technical and go far beyond the scope of this work. We will discuss them in detail in a forthcoming publication. Here, we state only a result for the terms containing the selective attraction–repulsion interaction in the order parameter equation. By using several approximations, such as homogeneous distribution of neighbours within the sensory range and small local order-parameter (close to the onset of collective motion), we obtain

$$-\frac{1}{s_0}\left(c(\mathbf{r}_i,t)\langle\sin(\varphi_i)\mathbf{F}_i\mathbf{e}_{\varphi_i}\rangle - s(\mathbf{r}_i,t)\langle\cos(\varphi_i)\mathbf{F}_i\mathbf{e}_{\varphi_i}\rangle\right) \approx \frac{\mu_\mathrm{m}-\mu_\mathrm{a}}{2}\Phi^2(\mathbf{r}_i,t). \tag{3.6}$$

Inserting this result into the order parameter equation (3.4) yields a necessary condition for a growing order parameter, i.e. onset of collective motion, which reads

$$\mu_\mathrm{m} - \mu_\mathrm{a} > 2\frac{D_\varphi}{s_0^2}. \tag{3.7}$$

Thus, collective motion in the $\mu_\mathrm{a}\mu_\mathrm{m}$-space can emerge only above the line $\mu_\mathrm{m} = \mu_\mathrm{a} + 2D_\varphi/s_0^2$ (see also figures 3 and 4). This implies that the region of collective motion includes the escape and pursuit regime ($\mu_\mathrm{m} > 0$ and $\mu_\mathrm{a} < 0$). With increasing noise strength D_φ, the regime of collective motion is predicted to recede further into the escape–pursuit regime. In general, the above condition will not be sufficient for the emergence of collective motion, and we expect that the actual region of the parameter space exhibiting collective motion will be smaller than predicted by equation (3.7). In order to locate it more precisely, a more detailed analysis of the coarse-grained equations is required, which is beyond the scope of this work.

4. SIMULATION RESULTS

In this section, we proceed with the discussion of systematic numerical simulations of the model for varying interactions strengths ($-5 \leq \mu_\mathrm{a,m} \leq 5$), different densities ρ and noise strengths D_φ. They allow the characterization of the system behaviour in different regimes with respect to the onset of collective motion and the strength of density inhomogeneities. The coupled stochastic differential equations (2.1) and (2.2) describing the system were numerically integrated using the standard Euler scheme [47].

In the following, we will discuss our results in term of the dimensionless density $\rho_\mathrm{s} = Nl_\mathrm{s}^2/L^2$, rescaled by the sensory range, which is proportional to the average number of individuals per interaction zone for a homogeneous (random) spatial distribution.

We focus in particular on the question what combinations of μ_a, μ_m lead to large-scale collective motion. The degree of collective motion after the system reaches a steady state is measured by the well-known order parameter used in the analysis of Vicsek-type models, which corresponds to the centre of mass speed normalized by the preferred speed of individuals:

$$\langle\Phi\rangle_t = \frac{1}{s_0}\langle|\langle\mathbf{v}_i\rangle_N|\rangle_t. \tag{4.1}$$

Here $\langle\cdot\rangle_t$ denotes the temporal average and $\langle\cdot\rangle_N$ the ensemble average. In addition, we measure the spatial inhomogeneity (clustering) by the time-averaged scaled neighbour number

$$\langle N\rangle_t = \left\langle \frac{\langle N_\mathrm{c}(t) + N_\mathrm{m}(t) + N_\mathrm{a}(t)\rangle_N}{N_\mathrm{max}} \right\rangle_t, \tag{4.2}$$

with $\langle N_\mathrm{c}(t) + N_\mathrm{m}(t) + N_\mathrm{a}(t)\rangle_N$ being the average number of neighbours within the metric distance given by the sensory range l_s of an individual at a given time t. The density-dependent scaling number N_max defines the maximal expectation values for the measured number of neighbours corresponding to the closest packing of individuals by assuming an impenetrable collision avoidance zone with a diameter l_c:

$$N_\mathrm{max} = \eta_{2d}\frac{4l_\mathrm{s}^2}{l_\mathrm{c}^2} - 1. \tag{4.3}$$

Here, $\eta_{2d} = \pi/(2\sqrt{3}) \approx 0.907$ is the packing fraction for the closest packing of discs in two spatial dimensions. The term -1 in the definition of N_max takes into account that the focal particle is not being counted as its own neighbour. Please note that as we are considering a soft core interaction, the clustering number $\langle N\rangle_t$ can, in principle, be larger than one, in particular for high densities and strong attraction.

Throughout this work, we set $s_0 = 1$, $l_\mathrm{c} = 1$ and $l_\mathrm{s} = 5$. Furthermore, we use $\mu_\mathrm{c} = 20$, which ensures that for binary interactions the short-ranged collision avoidance is always larger than the sum of the other possibly attracting forces. The particle number is set constant to $N = 2000$ and the density is varied by changing the system size L. The parameter-space diagrams in figures 3 and 4 were obtained from interpolating the results for $\langle\Phi\rangle_t$ and $\langle N\rangle_t$ for 441 (21×21) individual, evenly spaced, grid points in the interaction parameter space with $-5.0 \leq \mu_\mathrm{m}, \mu_\mathrm{a} \leq +5.0$. Each such point corresponds to an average over the results of six independent simulation runs, whereby for each run a temporal average was taken after the system reached a steady-state.

At sufficiently high densities and sufficiently low (angular) noise, we can observe the onset of collective motion for a range of interaction parameters, which coincides approximately with the escape and pursuit quadrant of the interaction parameter space with $\mu_\mathrm{m} > 0$ and $\mu_\mathrm{a} < 0$ (figures 3 and 4). It contains the special cases of only attraction to moving away (repulsion from approaching) individuals with $\mu_\mathrm{m} > 0$ and

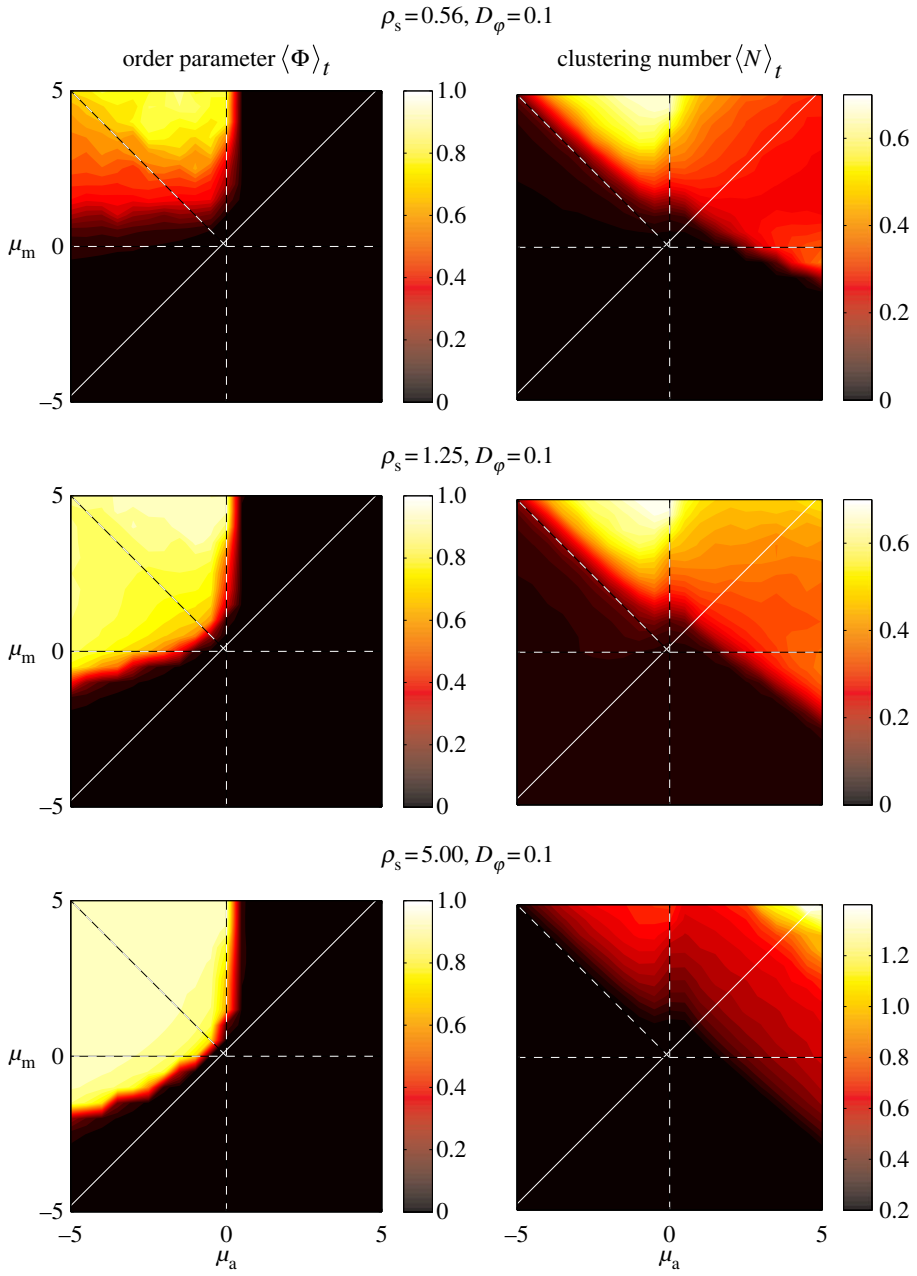

Figure 3. Steady-state order parameter $\langle \Phi \rangle_t$ (left) and clustering number $\langle N \rangle_t$ (right) versus μ_m and μ_a for different densities $\rho_s = 0.56$ (top), 1.25, 5.00 and $D_\varphi = 0.1$. The vertical and horizontal dashed lines indicate the zero axes. Equation (3.7) predicts the emergence of collective motion only above the solid diagonal line. The (diagonal) dashed lines in the escape and pursuit quadrant indicates the border between escape-dominated (below) and pursuit-dominated behaviour (above). Please note the different $\langle N \rangle_t$-scale used for clarity for $\rho = 5.00$.

$\mu_a = 0$ ($\mu_a < 0$ and $\mu_m > 0$), and extends also into the pure repulsion region ($\mu_a, \mu_m < 0$) and to a much lesser extent into the pure attraction region ($\mu_a, \mu_m > 0$ with $\mu_a \ll \mu_m$). This is in agreement with the predictions of the necessary condition derived from the coarse-grained theory (equation (3.7)). However, the region of collective motion is significantly smaller in simulations. This can be explained by the impact of spatial inhomogeneities, finite short-range repulsion and/or higher-order effects, which have been neglected in the derivation of the necessary condition for collective motion.

Within the escape and pursuit regime, where the repulsion to approaching individuals (escape) dominates over the attraction to moving away individuals (pursuit), the clustering number is low. This corresponds to a rather homogeneous spatial distribution of particles throughout the system. The clustering number $\langle N \rangle$ increases strongly in the pursuit-dominated regime ($|\mu_m| > |\mu_a|$ with $\mu_m > 0$, $\mu_a < 0$), indicating strong density inhomogeneities corresponding to dense collectively moving bands and clusters. This resembles the behaviour observed in the original Brownian particle escape and pursuit model.

The neighbour number is also high in the pure attraction regime ($\mu_a, \mu_m > 0$) without collective motion, where clusters with vanishing centre of mass velocity ($\Phi \approx 0$) can be observed. Interestingly, at moderate densities ($\rho_s = 0.56$, 1.25 in figures 3 and 4), the

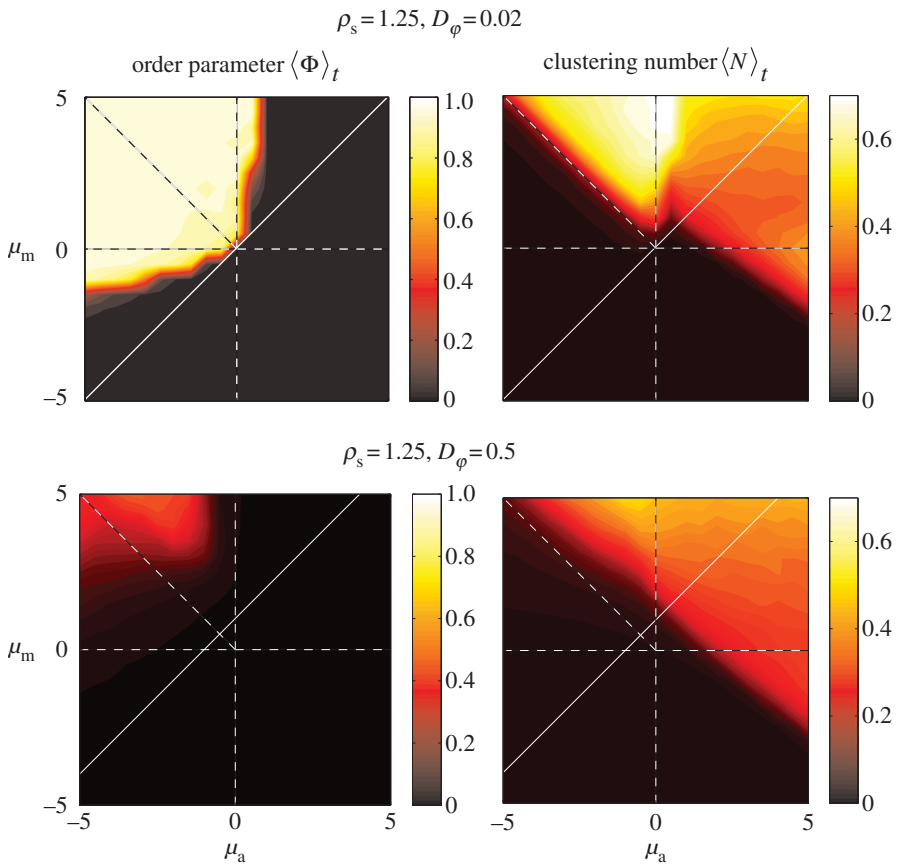

Figure 4. Steady-state order parameter $\langle \Phi \rangle_t$ (left) and the clustering number $\langle N \rangle_t$ (right) versus μ_m and μ_a for low angular noise $D_\varphi = 0.02$ (top) and high angular noise $D_\varphi = 0.5$ (bottom); lines as in figure 3.

maximum of the clustering number is located in the pursuit-dominated regime with collective motion, and not, as one might expect, in the regime of (strong) overall attraction ($\mu_m, \mu_a \gg 0$). In the ordered state, particles move approximately in the same direction and the relative speed $|\tilde{v}_{ji}|$ will be close to zero. For low repulsion from approaching individuals, the escape response is negligible, whereas the attraction to moving away individual suffices to maintain cohesion, in particular at low noise strengths. Effectively, the density of such collectively moving cluster is only limited by short-range repulsion, leading to the emergence of dense structures (figure 5*b*). In the pure attraction regime, particles on the boundaries of a cluster will be attracted towards the local centre of mass. However, owing to the self-propelled motion with inertia and scattering with other individuals within the disordered cluster, they will eventually move outwards again. As a result, we observe disordered aggregates, which resemble mosquito swarms (figure 2*b*), and are more dilute in comparison with the coherently moving clusters in the pursuit-dominated case.

As might be expected, increased stochasticity in the motion of individuals inhibits the onset of collective motion. The region of parameter space with $\langle \Phi \rangle_t$ significantly larger than 0 reduces strongly with increasing D_φ by receding towards the regime of strong escape and pursuit response (figure 4), in agreement with the kinetic theory.

For the head-on-head regime as well as for pure repulsion (with $\mu_m \gg 0$), a quasi-homogeneous distribution of particles can be observed with no collective motion (figures 2*c*,*d*, 3 and 4).

5. DISCUSSION

In this work, we have analysed a model for collective dynamics based on selective attraction and repulsion interactions, which was recently used to model the evolution of phenotypic phase change in locusts [42]. The modelling of individual dynamics in terms of stochastic differential equation (Langevin equations) allows a straight forward derivation of a coarse-grained description on the population level, which may be used for further theoretical analysis based on mean-field considerations and moment expansion of the corresponding PDF [45,46].

The model is able to account for three types of social responses relevant in the biological context: escape and pursuit, pure avoidance and pure attraction behaviour. Pure attraction may be associated with the selfish-herd effect [1], where individuals aggregate in order to reduce their individual risk from predation. Pure repulsion behaviour, on the other hand, represents a reasonable social response if close proximity to conspecifics is disadvantageous, for example, owing to the risk of cannibalism [39,42] or in the presence of strong competition for resources. Finally, we have shown that in the escape and pursuit regime, large-scale collective motion emerges without any explicit velocity-alignment mechanism. This parameter regime can be seen as a

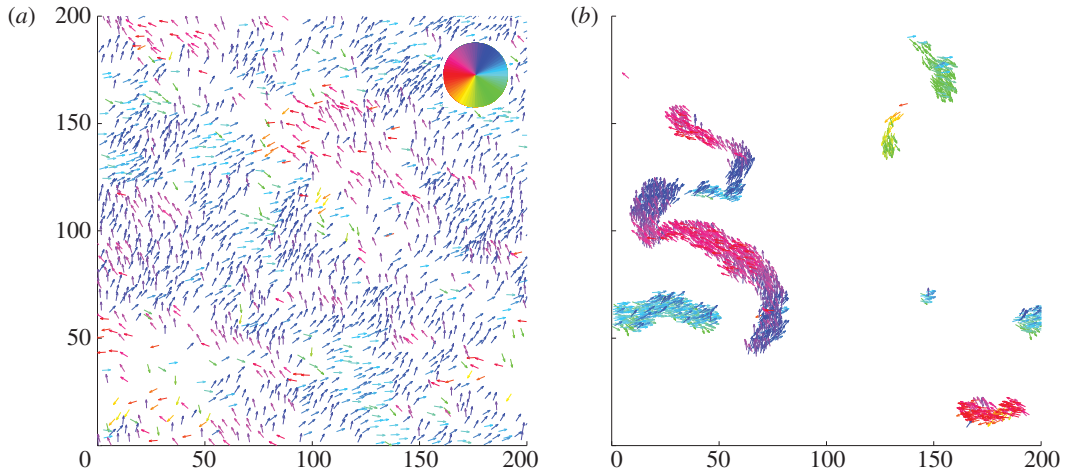

Figure 5. Examples of spatial configurations for (*a*) the pure escape case with $\mu_a = -3$ and $\mu_m = 0$, and (*b*) the pure pursuit case with $\mu_a = 0$ and $\mu_m = +3$.

generalization of the original escape and pursuit model motivated by empirical observations in locusts and Mormon crickets. We believe that the relevance of escape and pursuit is not restricted to the collective migration in insects, but that such a selective attraction–repulsion response represents an effective mechanism for onset of collective motion in various species, where the individual response relies on visual information. This conjecture has recently received further support from inference of social interactions from experimental data in fish [24,25].

Our results show that collective motion of self-propelled agents may emerge without the spatial anisotropy in the social interaction present in the original escape and pursuit model [12]. However, we would like to emphasize that in the original escape–pursuit model with Brownian agents, this spatial anisotropy is essential for the emergence of large-scale collective motion. This is related to the absence of an explicit self-propulsion in the dynamics of individuals in Romanczuk *et al.* [12], and the corresponding low persistence length in individual motion.

In general, the spatial distribution of individuals during collective motion depends strongly on the relative strength of the different social forces. If escape dominates, we observe a rather homogeneous spatial distribution (figure 5*a*), whereas in the pursuit-dominated case, compact, coherently moving structures, as for example snake-like clusters, can be observed (figure 5*b*). In between, for comparable escape and pursuit strengths, the band-like structures perpendicular to the average direction of motion emerge, which appear also in systems with velocity alignment (figure 2*a*) [9,13].

The region of collective motion decreases with increasing noise as well as with decreasing density. However, at low densities, the region of collective motion shows a clear shift towards the pursuit-dominated regime (figure 3, top), where, in a finite system, a non-vanishing order is maintained by relatively few moving clusters containing most of the individuals.

The emergence of polarized collective motion with non-vanishing order parameter in the escape–pursuit regime agrees with the qualitative prediction, drawn from the kinetic theory in §3. Furthermore, the general spatial patterns resemble the qualitative behaviour of the original escape–pursuit model [12]. Interestingly, at intermediate densities and within the interaction range studied, the strongest clustering in the system appears in the pursuit-dominated regime and not for pure attraction. This can be understood from the fact that local order decreases the effective 'temperature' associated with absolute deviations of the velocities of single particles from the average velocity of their neighbours [44–46]. As a result, we observe a decrease in the active pressure resulting from the stochastic self-propelled nature of individual motion, which counteracts the concentration of individuals due to attractive forces.

In conclusion, the modelling of collective motion in biology via selective attraction–repulsion interactions appears very promising. The model accounts for various individual behaviours and displays different spatial patterns of collective motion. The response based only on the distinction between approaching and moving away individuals can be directly linked to the response to looming visual stimuli, which has been shown to play an important role in various species [48,49,50]. Finally, in this context, we emphasize again the recent work by Lemasson & co-workers [36], where the authors introduce a model for collective motion based on selective interaction of individuals, using explicitly a simplified description of visual information available to each individual.

P.R. thanks V. Guttal (Indian Institute of Science) and I. D. Couzin (Princeton University) for many helpful discussions on the subject. Part of the work was done during a stay of L.S.G. at IFISC in Palma de Mallorca. L.S.G. thanks for the great hospitality and the fruitful cooperation. Furthermore, L.S.G. acknowledges the support by the DFG via the IRTG 1740.

REFERENCES

1 Hamilton, W. 1971 Geometry for the selfish herd. *J. Theor. Biol.* **31**, 295–311. (doi:10.1016/0022-5193(71)90189-5)

2 Couzin, I. D., Krause, J., James, R., Ruxton, G. D. & Franks, N. R. 2002 Collective memory and spatial sorting

in animal groups. *J. Theor. Biol.* **218**, 1–11. (doi:10.1006/jtbi.2002.3065)
3 Krause, J. & Ruxton, G. D. 2002 *Living in groups*. Oxford, UK: Oxford University Press.
4 Yates, C. A., Erban, R., Escudero, C., Couzin, I. D., Buhl, J., Kevrekidis, I. G., Maini, P. K. & Sumpter, D. J. T. 2009 Inherent noise can facilitate coherence in collective swarm motion. *Proc. Natl Acad. Sci. USA* **106**, 5464–5469. (doi:10.1073/pnas.0811195106)
5 Bazazi, S., Romanczuk, P., Thomas, S., Schimansky-Geier, L., Hale, J. J., Miller, G. A., Sword, G. A., Simpson, S. J. & Couzin, I. D. 2011 Nutritional state and collective motion: from individuals to mass migration. *Proc. R. Soc. B* **278**, 356–363. (doi:10.1098/rspb.2010.1447)
6 Vicsek, T., Czirók, A., Ben-Jacob, E., Cohen, I. & Shochet, O. 1995 Novel type of phase transition in a system of self-driven particles. *Phys. Rev. Lett.* **75**, 1226–1229. (doi:10.1103/PhysRevLett.75.1226)
7 Toner, J. & Tu, Y. 1995 Long-range order in a two-dimensional dynamical XY model: how birds fly together. *Phys. Rev. Lett.* **75**, 4326–4329. (doi:10.1103/PhysRevLett.75.4326)
8 Toner, J. & Tu, Y. 1998 Flocks, herds, and schools: a quantitative theory of flocking. *Phys. Rev. E* **58**, 4828–4858. (doi:10.1103/PhysRevE.58.4828)
9 Grégoire, G. & Chaté, H. 2004 Onset of collective and cohesive motion. *Phys. Rev. Lett.* **92**, 025702. (doi:10.1103/PhysRevLett.92.025702)
10 Aldana, M., Dossetti, V., Huepe, C., Kenkre, V. M. & Larralde, H. 2007 Phase transitions in systems of self-propelled agents and related network models. *Phys. Rev. Lett.* **98**, 095702. (doi:10.1103/PhysRevLett.98.095702)
11 Chaté, H., Ginelli, F., Grégoire, G. & Raynaud, F. 2008 Collective motion of self-propelled particles interacting without cohesion. *Phys. Rev. E* **77**, 046113. (doi:10.1103/PhysRevE.77.046113)
12 Romanczuk, P., Couzin, I. D. & Schimansky-Geier, L. 2009 Collective motion due to individual escape and pursuit response. *Phys. Rev. Lett.* **102**, 010602. (doi:10.1103/PhysRevLett.102.010602)
13 Romanczuk, P., Bär, M., Ebeling, W., Lindner, B. & Schimansky-Geier, L. 2012 Active Brownian particles. *Eur. Phys. J. Spec. Top.* **202**, 1951–6401. (doi:10.1140/epjst/e2012-01529-y)
14 Leonard, N., Paley, D., Lekien, F., Sepulchre, R., Fratantoni, D. & Davis, R. 2007 Collective motion, sensor networks, and ocean sampling. *Proc. IEEE* **95**, 48–74. (doi:10.1109/JPROC.2006.887295)
15 Sepulchre, R., Paley, D. & Leonard, N. 2008 Stabilization of planar collective motion with limited communication. *IEEE Trans. Autom. Control* **53**, 706–719. (doi:10.1109/TAC.2008.919857)
16 Turgut, A., Çelikkanat, H., Gökçe, F. & Şahin, E. 2008 Self-organized flocking in mobile robot swarms. *Swarm Intell.* **2**, 97–120. (doi:10.1007/s11721-008-0016-2)
17 Ferrante, E., Turgut, A., Mathews, N., Birattari, M. & Dorigo, M. 2011 Flocking in stationary and nonstationary environments: a novel communication strategy for heading alignment. In *Parallel problem solving from nature: PPSN XI* (eds R. Schaefer, C. Cotta, J. Kolodziej & G. Rudolph). Lecture Notes in Computer Science, no. 6239, pp. 331–340. Berlin, Germany: Springer.
18 Cucker, F. & Smale, S. 2007 Emergent behavior in flocks. *IEEE Trans. Autom. Control* **52**, 852–862. (doi:10.1109/TAC.2007.895842)
19 Carrillo, J. A., Fornasier, M., Toscani, G. & Vecil, F. Mathematical modeling of collective behavior in socio-economic and life sciences. *In Modeling and simulation in science, engineering and technology* (eds G. Naldi, L. Pareschi, G. Toscani & N. Bellomo), pp. 297–336. Boston: Birkhäuser.
20 Niwa, H. 1994 Self-organizing dynamic model of fish schooling. *J. Theor. Biol.* **171**, 123–126. (doi:10.1006/jtbi.1994.1218)
21 Couzin, I. D., Krause, J., Franks, N. R. & Levin, S. A. 2005 Effective leadership and decision making in animal groups on the move. *Nature* **433**, 513–516. (doi:10.1038/nature03236)
22 Romanczuk, P., Erdmann, U., Engel, H. & Schimansky-Geier, L. 2008 Beyond the Keller–Segel model microscopic modelling of bacterial colonies. *Eur. Phys. J. Spec. Top.* **157**, 61–77. (doi:10.1140/epjst/e2008-00631-1)
23 Bode, N. W. F., Franks, D. W. & Wood, J. A. 2010 Making noise. Emergent stochastic noise in a self propelled particle model. *J. Theor. Biol.* **267**, 292–299. (doi:10.1016/j.jtbi.2010.08.034)
24 Herbert-Read, J. E., Perna, A., Mann, R. P., Schaerf, T. M., Sumpter, D. J. T. & Ward, A. J. W. 2011 Inferring the rules of interaction of shoaling fish. *Proc. Natl Acad. Sci. USA* **108**, 18 726–18 731.(doi:10.1073/pnas.1109355108).
25 Katz, Y., Tunstrøm, K., Ioannou, C. C., Huepe, C. & Couzin, I. D. 2011 Inferring the structure and dynamics of interactions in schooling fish. *Proc. Natl Acad. Sci. USA* **108**, 18 720–18 725.(doi:10.1073/pnas.1107583108)
26 Breder, C. M. 1954 Equations descriptive of fish schools and other animal aggregations. *Ecology* **35**, 361–370. (doi:10.2307/1930099)
27 Romey, W. L. 1996 Individual differences make a difference in the trajectories of simulated schools of fish. *Ecol. Model.* **92**, 65–77. (doi:10.1016/0304-3800(95)00202-2)
28 Viscido, S. V., Parrish, J. K. & Grünbaum, D. 2005 The effect of population size and number of influential neighbors on the emergent properties of fish schools. *Ecol. Model.* **183**, 347–363. (doi:10.1016/j.ecolmodel.2004.08.019)
29 Ebeling, W. & Schweitzer, F. 2001 Swarms of particle agents with harmonic interactions. *Theory Biosci.* **120**, 207–224.
30 Erdmann, U., Ebeling, W. & Mikhailov, A. S. 2005 Noise-induced transition from translational to rotational motion of swarms. *Phys. Rev. E* **71**, 051904. (doi:10.1103/PhysRevE.71.051904)
31 Peruani, F., Deutsch, A. & Bär, M. 2006 Nonequilibrium clustering of self-propelled rods. *Phys. Rev. E* **74**, 030904. (doi:10.1103/PhysRevE.74.030904)
32 Grossman, D., Aranson, I. S. & Jacob, E. B. 2008 Emergence of agent swarm migration and vortex formation through inelastic collisions. *New J. Phys.* **10**, 023036. (doi:10.1088/1367-2630/10/2/023036)
33 Strefler, J., Erdmann, U. & Schimansky-Geier, L. 2008 Swarming in three dimensions. *Phys. Rev. E* **78**, 031927. (doi:10.1103/PhysRevE.78.031927)
34 Strömbom, D. 2011 Collective motion from local attraction. *J. Theor. Biol.* **283**, 145. (doi:10.1016/j.jtbi.2011.05.019)
35 Steele, A. J., Tinsley, M. & Showalter, K. 2008 Collective behavior of stabilized reaction–diffusion waves. *Chaos* **18**, 026108. (doi:10.1063/1.2900386)
36 Lemasson, B., Anderson, J. & Goodwin, R. 2009 Collective motion in animal groups from a neurobiological perspective: the adaptive benefits of dynamic sensory loads and selective attention. *J. Theor. Biol.* **261**, 501–510. (doi:10.1016/j.jtbi.2009.08.013)
37 Moussaid, M., Helbing, D. & Theraulaz, G. 2011 How simple rules determine pedestrian behavior and crowd disasters? *Proc. Natl Acad. Sci. USA* **108**, 6884–6888. (doi:10.1073/pnas.1016507108)
38 Simpson, S. J., Sword, G. A., Lorch, P. D. & Couzin, I. D. 2006 Cannibal crickets on a forced march for protein and

salt. *Proc. Natl Acad. Sci. USA* **103**, 4152–4156. (doi:10.1073/pnas.0508915103)
39 Bazazi, S., Buhl, J., Hale, J. J., Anstey, M. L., Sword, G. A., Simpson, S. J. & Couzin, I. D. 2008 Collective motion and cannibalism in locust migratory bands. *Curr. Biol.* **18**, 735–739. (doi:10.1016/j.cub.2008.04.035)
40 Kamimura, A. & Ohira, T. 2010 Group chase and escape. *New J. Phys.* **12**, 053013. (doi:10.1088/1367-2630/12/5/053013)
41 Sengupta, A., Kruppa, T. & Löwen, H. 2011 Chemotactic predator–prey dynamics. *Phys. Rev. E* **83**, 031914. (doi:10.1103/PhysRevE.83.031914)
42 Guttal, V., Romanczuk, P., Simpson, S. J., Sword, G. A. & Couzin, I. D. 2012 Cannibalism can drive the evolution of behavioural phase polyphenism in locusts. *Ecol. Lett.* **15**, 1158–1166. (doi:10.1111/j.1461-0248.2012.01840.x)
43 Couzin, I. D., Ioannou, C. C., Demirel, G., Gross, T., Torney, C. J., Hartnett, A., Conradt, L., Levin, S. A. & Leonard, N. E. 2011 Uninformed individuals promote democratic consensus in animal groups. *Science* **334**, 1578–1580, (doi:10.1126/science.1210280)
44 Romanczuk, P. & Erdmann, U. 2010 Collective motion of active Brownian particles in one dimension. *Eur. Phys. J. Spec. Top.* **187**, 127–134. (doi:10.1140/epjst/e2010-01277-0)
45 Romanczuk, P. & Schimansky-Geier, L. 2011 *Ecol. Complex.* **10**, 83–92. (doi:10.1016/j.ecocom.2011.07.008)
46 Grossmann, R., Schimansky-Geier, L. & Romanczuk, P. 2012 Active Brownian particles with velocity-alignment and active fluctuations. *New J. Phys.* (http://arxiv.org/abs/1204.4304)
47 Mannella, R. 2000 A gentle introduction to the integration of stochastic differential equations. In *Stochastic processes in physics, chemistry, and biology*, vol. 557 (eds J. Freund & T. Poeschel). Lecture Notes in Physics, pp. 353–364. Berlin/Heidelberg: Springer.
48 Schiff, W., Caviness, J. A. & Gibson, J. J. 1962 Persistent fear responses in Rhesus monkeys to the optical stimulus of 'looming'. *Science* **136**, 982–983. (doi:10.1126/science.136.3520.982)
49 Rind, F. C. & Simmons, P. J. 1992 Orthopteran DCMD neuron: a reevaluation of responses to moving objects. I. Selective responses to approaching objects. *J. Neurophysiol.* **68**, 1654–1666.
50 de Vries, S. & Clandinin, T. 2012 Loom-sensitive neurons link computation to action in the *Drosophila* visual system. *Curr. Biol.* **22**, 353–362. (doi:10.1016/j.cub.2012.01.007)